Determination of Critical Properties and Acentric Factors of Petroleum Fractions Using Artificial Neural Networks

ARTICLE *in* INDUSTRIAL & ENGINEERING CHEMISTRY RESEARCH · APRIL 2008

Impact Factor: 2.59 · DOI: 10.1021/ie0712378

3 AUTHORS:

Amir H. Mohammadi

550 PUBLICATIONS **4,800** CITATIONS

SEE PROFILE

Waheed Afzal

University of Aberdeen

49 PUBLICATIONS **366** CITATIONS

SEE PROFILE

Dominique Richon

Aalto University

532 PUBLICATIONS **6,591** CITATIONS

SEE PROFILE

GENERAL RESEARCH

Determination of Critical Properties and Acentric Factors of Petroleum Fractions Using Artificial Neural Networks

Amir H. Mohammadi, Waheed Afzal, and Dominique Richon*

Mines Paris, ParisTech, CEP-TEP, CNRS FRE 2861, 35 Rue Saint Honoré, 77305 Fontainebleau, France

Various correlations are available that can determine the critical properties and acentric factors of petroleum fractions. The available methods may have low accuracy in determining these properties for heavy petroleum fractions and may require further verification because, during the development of the original predictive methods, the data describing the critical properties and acentric factors of heavy hydrocarbons and petroleum fractions were not available. In this work, after a quick review of the most common correlations reported in the literature, an alternative method based on the artificial neural network (ANN) technique is proposed to predict the critical temperatures, critical pressures, critical volumes, and acentric factors of petroleum fractions, especially heavy fractions, from their specific gravity and the average normal boiling-point temperature values. Among the different neural networks reported in the literature, the feed-forward neural network method with a modified Levenberg−Marquardt optimization algorithm is used. The model is trained and tested using the data recommended in the literature for critical properties and acentric factors of C_1-C_{45} petroleum fractions. Independent data (not used in training and developing the model) are used to validate and examine the reliability of this tool. The predictions of this model are found in acceptable agreement with the data recommended in the literature, demonstrating the reliability of the ANN technique used in this work.

1. Introduction

Petroleum fluids are composed mainly of hydrocarbon constituents. The behavior of these fluids is determined by their chemical composition and the prevailing temperature and pressure. This behavior is of a prime consideration in the development and management of petroleum industry, affecting all aspects of petroleum production, transportation, and processing.[1] Real petroleum fluids could be composed of thousands of components, which pose two major restrictions:[1] (1) A full description of the fluid by identifying all of its constituents may not be possible. (2) Phase-behavior calculations for systems defined by a large number of components are time-consuming and particularly impractical in compositional modeling.[1] An oil or condensate is commonly described by discrete hydrocarbon components up to C_6 and the non-hydrocarbon gases, such as N_2, CO_2, and H_2S and hydrocarbon groups for heavier fractions. The concentration of certain major nonparaffin constituents, within the C_6 to C_9 groups, such as, benzene, toluene, cyclohexane, and xylene, may also be identified.[1] The hydrocarbon groups are generally determined according to their boiling point temperatures by distillation and/or gas chromatography.[1]

The distilled hydrocarbon groups are characterized by measuring some of their properties such as the average normal boiling-point temperature, molecular weight, and density.[1] These properties are used in generalized correlations to estimate other properties, such as the critical temperature (T_c), critical pressure (P_c), critical volume (V_c), and the acentric factor (ω), which are required for phase-behavior modeling using equations of state.[1] These properties are normally determined from generalized correlations in terms of the average normal boiling point (T_b), the specific gravity (S) at 288.7 K (15.5 °C or 60 °F) or molecular weight (M) of petroleum fractions.[1] These groups, which are called single carbon number (SCN) groups, are fractions that are commonly collected within the temperature range of two consecutive normal alkanes, where each cut begins and ends at the boiling point of normal C_{n-1} and normal C_n, respectively, and is referred to by the carbon number n.[1] The majority of these correlations have been reported by Ahmed.[2] The most widely used have been reviewed by Danesh,[1] which are summarized in the Appendix.[1] The correlations are for single carbon group properties, and their application to very wide boiling range fractions such as C_{7+} is not recommended.[1]

Most of the existing correlations have normally been reported based on the data for pure and light hydrocarbons and, hence, may not be accurate for determining the critical properties and the acentric factors of heavy petroleum fractions. Therefore, there is still a need for robust methods to determine these properties. In this work, the capability of ANNs to estimate the critical properties and acentric factors of petroleum fractions from their specific gravities and average normal boiling-point temperatures is shown. To our knowledge, such a technique has not already been applied to determine these properties for petroleum fractions. Among the various ANNs reported in the literature, the feed-forward (back-propagation) neural network (FNN) method[3] with a modified Levenberg−Marquardt optimization algorithm[4−6] is used, which is known to be effective to represent the nonlinear relationships between variables in complex systems.[2,7−16] To develop this model, the data recommended in the literature data[1] on the critical properties and acentric factors of C_1-C_{45} petroleum fractions are used. The developed model is then employed to predict independent data (not used in the training and developing the *ANN* model). It is shown that the results of the *ANN* model are in acceptable agreement with the data, demonstrating the capability of this

* To whom correspondence should be addressed. Tel.: +(33) 1 64 69 49 65. Fax: +(33) 1 64 69 49 68. E-mail: richon@ensmp.fr.

10.1021/ie0712378 CCC: $40.75
Published on Web 04/05/2008

tool to determine the critical properties and acentric factors of petroleum fractions.

2. Artificial Neural Network

ANNs have large numbers of computational units called neurons, connected in a massively parallel structure, and do not need an explicit formulation of the mathematical or physical relationships of the handled problem.[2,7−16] The most commonly used ANNs are the feed-forward neural networks,[10] which are designed with one input layer, one output layer, and hidden layers.[2,7−16] The number of neurons in the input and output layers equals to the number of 'inputs' and 'outputs' physical quantities, respectively. The disadvantage of FNNs is the determination of the ideal number of neurons in the hidden layer(s); few neurons produce a network with low precision, and a higher number leads to overfitting and bad quality of interpolation and extrapolation. *The use of techniques such as Bayesian regularization, along with a Levenberg−Marquardt algorithm, can help overcome this problem.*[4−6]

In the FNN method, the input layer of the network receives all the input data and introduces scaled data to the network. The data from the input neurons are propagated through the network via weighted interconnections. Every *i* neuron in a *k* layer is connected to every neuron in adjacent layers. The *i* neuron within the hidden *k* layer performs the following tasks: summation of the arriving weighted inputs (input vector $I_i = [I_{i,1},...I_{i,Nk-1}]$) and propagations of the resulting summation through a nonlinear activation function, *f*, to the adjacent neurons of the next hidden layer or to the output neuron(s).[12] The exponential sigmoid transfer function is normally used:[12]

$$f(x) = \frac{1}{1+e^{-x}} \qquad \text{where } x \in [0,1] \tag{1}$$

where *x* stands for parameter of nonlinear activation function. A bias term, *b*, is associated with each interconnection to introduce a supplementary degree of freedom. The expression of the weighted sum, *S′*, to the *i*th neuron in the *k*th layer ($k \geq 2$) is:[12]

$$S'_{k,i} = \sum_{j=1}^{N_{k-1}} [(w_{k-1,j,i} I_{k-1,j}) + b_{k,i}] \tag{2}$$

where *w* is the weight parameter between each neuron−neuron interconnection. Using this simple feed-forward network with nonlinear sigmoid activation function, the output, *O*, of the *i* neuron within the hidden *k* layer is:[12]

$$O_{k,i} = \frac{1}{1+e^{-(\sum_{j=1}^{N_{k-1}}[(w_{k-1,j,i}I_{k-1,j})+b_{k,i}])}} = \frac{1}{1+e^{-S'_{k,i}}} \tag{3}$$

To develop the ANN, the data sets are subdivided into three classes: training, testing, and validation.[12] After partitioning the data sets, the training set is used to tune the parameters. All of the synaptic weights and biases are first initialized randomly.[12] The network is then trained; its synaptic weights are adjusted by an optimization algorithm until it correctly emulates the input/output mapping, by minimizing the average root-mean-square error.[12] The optimization method chosen in this work was the Levenberg−Marquart algorithm[4−6] along with Bayesian regularization technique, as mentioned earlier. This algorithm is specially indicated to optimize ANNs using small learning sample size.[13−16] The testing set is used during the adjustment of the network's synaptic weights to evaluate the algorithms performance on the data not used for tuning and stop the tuning if the error on the testing set increases.[12] Finally, the validation set measures the generalization ability of the model after the fitting process.[12]

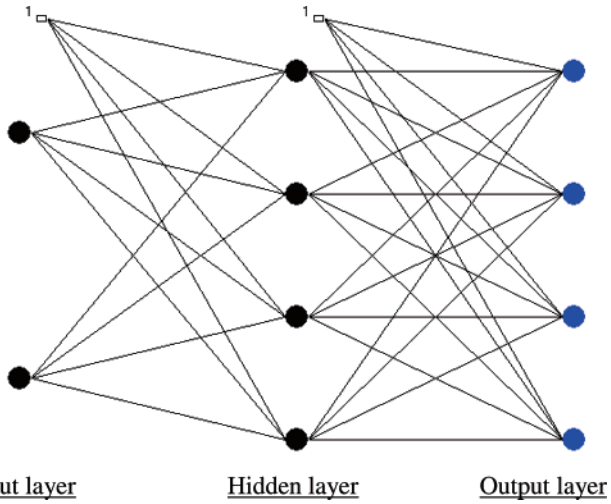

Figure 1. Topology of the neural network model used to calculate/predict the critical properties and acentric factors of petroleum fractions (1, bias; ●, neuron). Output neurons are the ratio of the critical temperature to the average normal boiling-point temperature, critical pressure, critical volume, and acentric factor; input neurons are specific gravity and normal boiling-point temperature.

Table 1. Number of Neurons, Hidden Layers, Parameters, and Data Used in This Model for Calculating/Predicting the Critical Properties and Acentric Factors of Petroleum Fractions[a]

layer	number of neurons
1	2
2	4
3	4

[a] Number of hidden layers = 1; number of parameters = 32; number of data used for training = 44; number of data used for testing = 5; number of data used for validation = 18; type of activation function, exponential sigmoid.

3. Results and Discussion

The ANN model shown in Figure 1 and detailed in Table 1, with one hidden layer, was used for the computation of the critical pressure, critical volume, acentric factor, and the ratioof the critical temperature to average normal boiling-point temperature as a function of the specific gravity and average normal boiling-point temperature of C_1-C_{45} petroleum fractions. *To have similar order of magnitudes for the numerical values of the outputs, the ratio of the critical temperature to the average normal boiling-point temperature was used rather than the critical temperature.* Furthermore, because experimental measurements of the specific gravity and average normal boiling-point temperature for hydrocarbons, especially petroleum fluids are easier than molecular weight measurements, therefore the specific gravity and average normal boiling-point temperature were used as inputs to estimate the critical properties and the acentric factors of petroleum fractions. The pseudo-experimental data[1] shown in Table 2 were used for training (and testing). *As can be observed, the single carbon numbers cover the practical range for compositional analysis, i.e., from C_1 to C_{45}.* The best value of the number of the hidden neurons according to both the accuracy of the fit (minimum value of the objective function) and the predictive power of the neural network was found to be 4.

Table 2 also shows the absolute deviations (AD) and average absolute deviations (AAD) between the pseudo-experimental[1]

Table 2. Comparison of Critical Temperatures (T_c), Critical Pressures (P_c), Critical Volumes (V_c), and Acentric Factors (ω) Calculated by the ANN Model with Those Recommended in the Literature[1] for Different Petroleum Fractions

Petroleum Fraction	Input		Critical Properties and Acentric Factors											
			T_c/K			P_c/MPa			V_c/m^3·kmol^{-1}			ω		
	T_b/K	S	exp.[a]	cal.	AD%[b]	exp.	cal.	AD%	exp.	cal.	AD%	exp.	cal.	AD%
C_1	112	0.300	190.6	190.6	0.0	4.599	4.598	0.0	0.099	0.094	5.1	0.012	0.012	0.0
C_2	185	0.356	305.3	305.4	0.0	4.872	4.867	0.1	0.146	0.145	0.7	0.100	0.100	0.0
C_3	231	0.507	369.8	369.5	0.1	4.248	4.250	0.0	0.200	0.203	1.5	0.152	0.146	3.9
i-C_4	261	0.563	408.1	408.0	0.0	3.648	3.700	1.4	0.263	0.263	0.0	0.177	0.187	5.6
n-C_4	273	0.584	425.1	422.9	0.5	3.796	3.577	5.8	0.255	0.277	8.6	0.200	0.198	1.0
i-C_5	301	0.625	460.4	459.9	0.1	3.381	3.345	1.1	0.306	0.316	3.3	0.228	0.228	0.0
Ne−C_5[c]	283	0.597	433.8	435.8	0.5	3.199	3.479	8.8	0.304	0.293	3.6	0.196	0.210	7.1
N−C_5	309	0.631	469.7	469.7	0.0	3.370	3.266	3.1	0.313	0.332	6.1	0.252	0.242	4.0
n-C_6[c]	342	0.664	507.6	509.3	0.3	3.025	3.013	0.4	0.371	0.389	4.9	0.301	0.286	5.0
C_6	337	0.690	509.9	509.7	0.0	3.271	3.225	1.4	0.348	0.339	2.6	0.251	0.249	0.8
C_7	366	0.727	547.2	546.4	0.1	3.071	3.062	0.3	0.392	0.376	4.1	0.280	0.278	0.7
C_8	390	0.749	574.1	574.3	0.0	2.877	2.885	0.3	0.433	0.419	3.2	0.312	0.311	0.3
C_9	416	0.768	603.2	602.7	0.1	2.665	2.677	0.5	0.484	0.473	2.3	0.352	0.353	0.3
C_{10}	439	0.782	626.9	626.6	0.0	2.481	2.493	0.5	0.532	0.526	1.1	0.389	0.392	0.8
C_{11}	461	0.793	649.1	648.6	0.1	2.310	2.320	0.4	0.584	0.580	0.7	0.429	0.433	0.9
C_{12}	482	0.804	670.0	669.4	0.1	2.165	2.172	0.3	0.635	0.633	0.3	0.467	0.472	1.1
C_{13}	501	0.815	688.9	688.4	0.1	2.054	2.052	0.1	0.681	0.679	0.3	0.501	0.506	1.0
C_{14}	520	0.826	708.2	707.2	0.1	1.953	1.943	0.5	0.727	0.726	0.1	0.536	0.540	0.7
C_{15}	539	0.836	727.1	725.6	0.2	1.853	1.839	0.8	0.777	0.775	0.3	0.571	0.576	0.9
C_{16}	557	0.843	743.0	742.4	0.1	1.752	1.741	0.6	0.830	0.828	0.2	0.610	0.614	0.7
C_{17}	573	0.851	758.1	757.6	0.1	1.679	1.666	0.8	0.874	0.872	0.2	0.643	0.646	0.5
C_{18}	586	0.856	770.0	769.5	0.1	1.614	1.605	0.6	0.915	0.911	0.4	0.672	0.675	0.4
C_{19}	598	0.861	781.0	780.6	0.1	1.559	1.552	0.4	0.951	0.948	0.3	0.698	0.701	0.4
C_{20}	612	0.866	793.2	793.2	0.0	1.495	1.492	0.2	0.997	0.993	0.4	0.732	0.733	0.1
C_{21}	624	0.871	803.7	804.1	0.0	1.446	1.444	0.1	1.034	1.031	0.3	0.759	0.761	0.3
C_{22}	637	0.876	814.7	815.7	0.1	1.393	1.394	0.1	1.077	1.074	0.3	0.789	0.791	0.3
C_{23}	648	0.881	824.9	825.7	0.1	1.356	1.355	0.1	1.110	1.109	0.1	0.815	0.816	0.1
C_{24}	659	0.885	834.3	835.5	0.1	1.314	1.318	0.3	1.147	1.145	0.2	0.841	0.842	0.1
C_{25}	671	0.888	844.1	845.4	0.2	1.263	1.271	0.6	1.193	1.193	0.0	0.874	0.876	0.2
C_{26}	681	0.892	853.3	854.1	0.1	1.230	1.238	0.7	1.226	1.228	0.2	0.897	0.900	0.3
C_{27}	691	0.896	861.7	862.7	0.1	1.200	1.206	0.5	1.259	1.263	0.3	0.944	0.925	2.0
C_{28}	701	0.899	869.9	871.0	0.1	1.164	1.173	0.8	1.296	1.301	0.4	0.968	0.951	1.8
C_{29}	709	0.902	877.0	877.8	0.1	1.140	1.149	0.8	1.323	1.330	0.5	0.985	0.971	1.4
C_{30}	719	0.905	885.1	886.0	0.1	1.107	1.117	0.9	1.361	1.368	0.5	1.008	0.998	1.0
C_{31}	728	0.909	893.3	893.7	0.0	1.085	1.092	0.6	1.389	1.398	0.6	1.026	1.019	0.7
C_{32}[c]	737	0.912	901.4	901.0	0.0	1.060	1.065	0.5	1.421	1.431	0.7	1.046	1.041	0.5
C_{33}	745	0.915	906.7	907.7	0.1	1.039	1.042	0.3	1.448	1.459	0.8	1.063	1.061	0.2
C_{34}	753	0.917	914.1	914.0	0.0	1.013	1.018	0.5	1.480	1.490	0.7	1.082	1.081	0.1
C_{35}	760	0.920	920.4	919.9	0.1	0.998	1.000	0.2	1.502	1.513	0.7	1.095	1.097	0.2
C_{36}	768	0.922	926.2	926.2	0.0	0.974	0.977	0.3	1.534	1.542	0.5	1.114	1.117	0.3
C_{37}	774	0.925	931.9	931.9	0.1	0.964	0.962	0.2	1.550	1.560	0.6	1.124	1.129	0.4
C_{38}	782	0.927	937.6	937.6	0.0	0.941	0.939	0.2	1.583	1.588	0.3	1.142	1.148	0.5
C_{39}	788	0.929	943.2	942.4	0.1	0.927	0.924	0.3	1.604	1.607	0.2	1.154	1.161	0.6
C_{40}	796	0.931	949.6	948.7	0.1	0.905	0.902	0.3	1.636	1.633	0.2	1.172	1.178	0.5
C_{41}	801	0.933	954.0	952.9	0.1	0.896	0.890	0.7	1.652	1.648	0.2	1.181	1.188	0.6
C_{42}	807	0.934	956.3	957.5	0.1	0.877	0.873	0.5	1.680	1.667	0.8	1.195	1.201	0.5
C_{43}[c]	813	0.936	964.2	962.4	0.2	0.864	0.858	0.7	1.701	1.684	1.0	1.207	1.212	0.4
C_{44}	821	0.938	969.6	968.7	0.1	0.844	0.838	0.7	1.733	1.707	1.5	1.224	1.227	0.2
C_{45}[c]	826	0.940	973.9	972.9	0.1	0.835	0.827	1.0	1.749	1.740	0.5	1.232	1.235	0.2
AAD%[d]					0.1			0.8			1.3			1.0

[a] (Pseudo-)experimental data have been reported by Danesh.[1] [b] AD = (|(experimental value − calculated value)/experimental value|). [c] These values have been used for testing. The rest of data have been used for training. [d] AAD = $((1/M)\sum_{i=1}^{M}$|(experimental value − calculated value)/experimental value|), where M represents number of (pseudo-)experimental points.

and calculated data. A preliminary study shows that the results should be acceptable enough because the input variables were well chosen (two input variables, i.e., S and T_b) and there were sufficient data to train the network. As can be observed, the ANN model yields acceptable results, especially for heavy petroleum fractions. The AADs% equal to 0.1, 0.8, 1.3, and 1.0 were obtained for the critical temperatures, critical pressures, critical volumes, and acentric factors, respectively. Figures 2−5 show the differences between the pseudo-experimental[1] and calculated values (coming from the ANN model) versus the pseudo-experimental[1] values for the critical temperatures, critical pressures, critical volumes, and acentric factors, respectively, reported in Table 2. As can be observed, the maximum differences between the pseudo-experimental[1] and calculated values are less than 2.5 K for the critical temperatures, less than 0.3 MPa for the critical pressures, less than 0.03 m^3·kmol^{-1} for the critical volumes, and 0.02 for the acentric factors, reconfirming that the ANN method results are quite acceptable.

The data on normal paraffins were then used for validation. *It should be mentioned that the use of this model, which has been developed for SCN groups, for normal paraffins may be conservative*, however, as can be seen in Table 3, acceptable results have been obtained. Table 3 shows the absolute deviations and average absolute deviations between the pseudo-experimental[1] and predicted data. As can be observed, the AADs% equal to 1, 8, 2.7, and 3 were obtained for the critical temperatures, critical pressures, critical volumes, and acentric factors, respectively, which are relatively acceptable. Figures

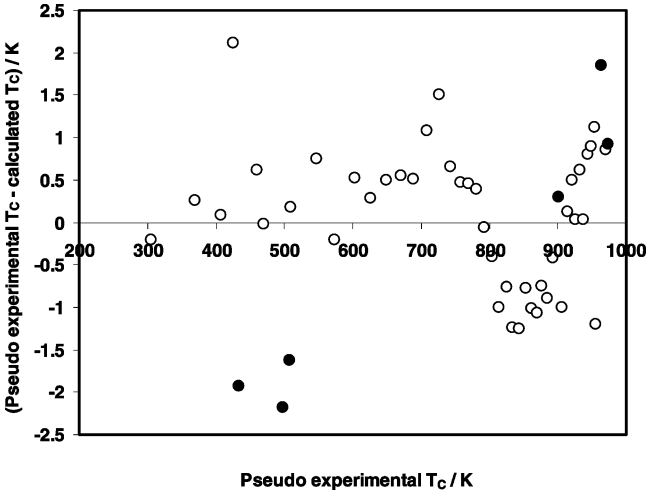

Figure 2. Difference between the pseudo-experimental value and the calculated value versus the pseudo-experimental value for critical temperature (T_c) of petroleum fraction. (○), data used for training; (●), data used for testing.

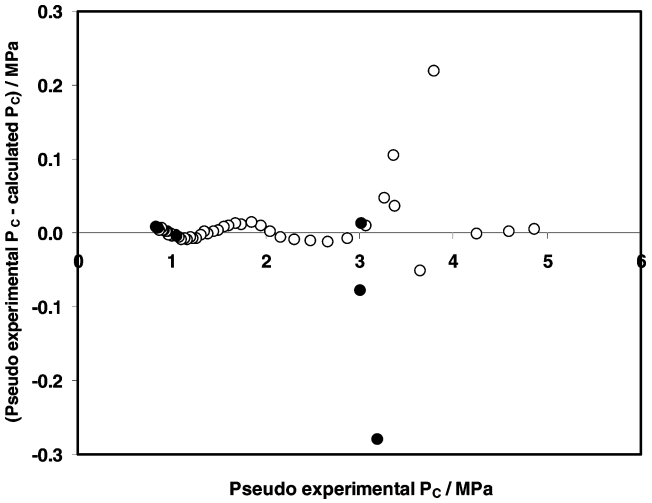

Figure 3. Difference between the pseudo-experimental value and the calculated value versus the pseudo-experimental value for critical pressure (P_c) of petroleum fraction. (○), data used for training; (●), data used for testing.

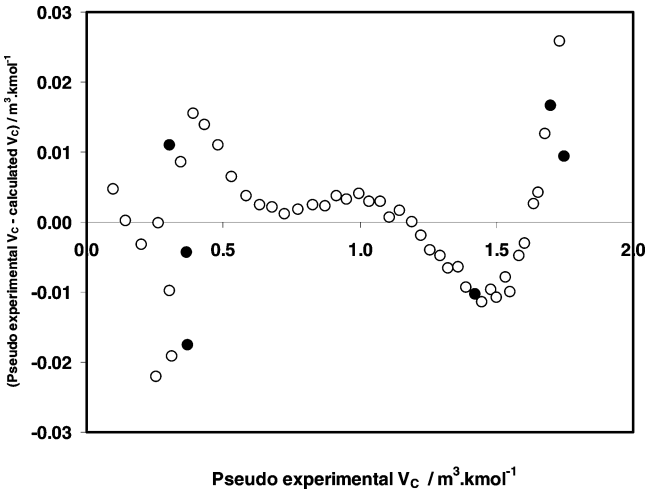

Figure 4. Difference between the pseudo-experimental value and the calculated value versus the pseudo-experimental value for critical volume (V_c) of petroleum fraction. (○), data used for training; (●), data used for testing.

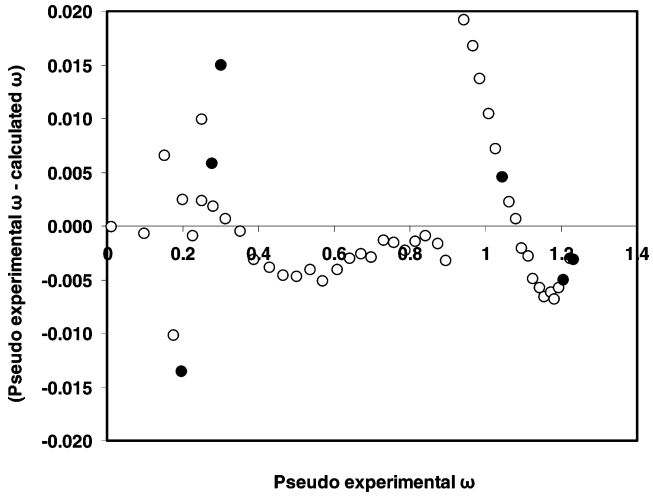

Figure 5. Difference between the pseudo-experimental value and the calculated value versus the pseudo-experimental value for acentric factor (ω) of petroleum fraction. (○), data used for training; (●), data used for testing.

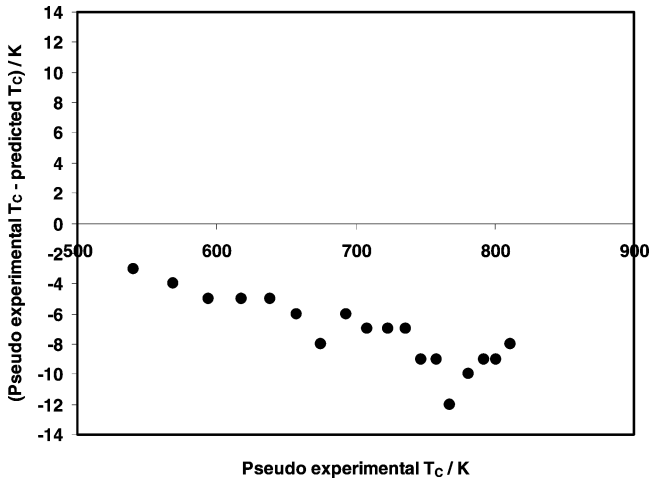

Figure 6. Difference between the pseudo-experimental value and the predicted value versus the pseudo-experimental value for the critical temperature of normal paraffin. (●) data used for validation.

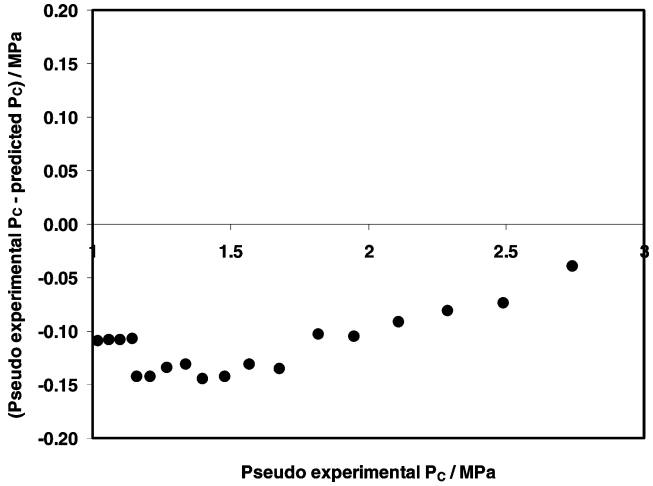

Figure 7. Difference between the pseudo-experimental value and the predicted value versus the pseudo-experimental value for critical pressure of normal paraffin. (●) data used for validation.

6−9 show the differences between the pseudo-experimental[1] and predicted values versus the pseudo-experimental[1] values for the critical temperatures, critical pressures, critical volumes, and acentric factors, respectively, reported in Table 3. As can

Table 3. Comparison of Critical Temperatures, Critical Pressures, Critical Volumes, and Acentric Factors Predicted by the ANN Model with Those Reported in the Literature[1] for Different Normal Paraffins[a]

Normal Paraffin	Input		Critical Properties and Acentric Factors											
			T_c/K			P_c/MPa			V_c/m^3·kmol^{-1}			ω		
	T_b/K	S	exp.[b]	pred.	*AD*%[c]	exp.	pred.	*AD*%	exp.	pred.	*AD*%	exp.	pred.	*AD*%
n-heptane	371.58	0.688	540	543	0.6	2.740	2.780	1.5	0.428	0.447	4.4	0.350	0.332	5.1
n-octane	398.83	0.707	569	573	0.7	2.490	2.564	3.0	0.486	0.507	4.3	0.400	0.378	5.5
n-nonane	423.97	0.722	595	599	0.7	2.290	2.371	3.5	0.544	0.567	4.2	0.444	0.423	4.7
n-docane	447.30	0.734	618	623	0.8	2.110	2.202	4.4	0.600	0.627	4.5	0.492	0.467	5.1
n-undecene	469.08	0.745	639	644	0.8	1.949	2.054	5.4	0.659	0.685	3.9	0.530	0.510	3.8
n-dodecane	489.47	0.753	658	664	0.9	1.820	1.923	5.7	0.716	0.743	3.8	0.576	0.553	4.0
n-tridecane	508.62	0.762	675	683	1.2	1.680	1.815	8.0	0.775	0.797	2.8	0.617	0.592	4.1
n-tetradecane	526.73	0.763	693	699	0.9	1.570	1.701	8.3	0.830	0.862	3.9	0.643	0.640	0.5
n-pentadecane	543.83	0.772	708	715	1.0	1.480	1.623	9.7	0.889	0.911	2.5	0.686	0.675	1.6
n-hexadecane	560.01	0.777	723	730	1.0	1.400	1.545	10.4	0.944	0.966	2.3	0.717	0.714	0.4
n-heptadecane	575.30	0.780	736	743	1.0	1.340	1.471	9.8	1.000	1.024	2.4	0.770	0.756	1.8
n-octadecane	589.86	0.782	747	756	1.2	1.270	1.404	10.6	1.060	1.081	2.0	0.811	0.797	1.7
n-nonadecane	603.05	0.787	758	767	1.2	1.210	1.353	11.8	1.120	1.127	0.6	0.852	0.830	2.6
n-eicosane	616.93	0.792	768	780	1.6	1.160	1.303	12.3	1.170	1.176	0.5	0.907	0.864	4.7
n-heicosane	629.70	0.795	782	791	1.2	1.147	1.254	9.3	1.198	1.227	2.4	0.922	0.900	2.4
n-docosane	641.80	0.798	792	801	1.1	1.101	1.209	9.8	1.253	1.275	1.8	0.955	0.934	2.2
n-tricosane	653.40	0.800	801	810	1.1	1.059	1.167	10.2	1.307	1.323	1.2	0.989	0.967	2.2
n-tetracosane	664.40	0.803	810	819	1.1	1.019	1.128	10.7	1.362	1.368	0.4	1.019	0.999	2.0
AAD%[d]					1.0			8.0			2.7			3.0

[a] All of the values have been used for validation. [b] (Pseudo-)experimental data have been reported by Danesh.[1] [c] AD = (|(experimental value − predicted value)/experimental value|). [d] AAD = $((1/M)\sum_{i=1}^{M}$ |(experimental value − predicted value)/experimental value|), where M represents number of (pseudo-) experimental points.

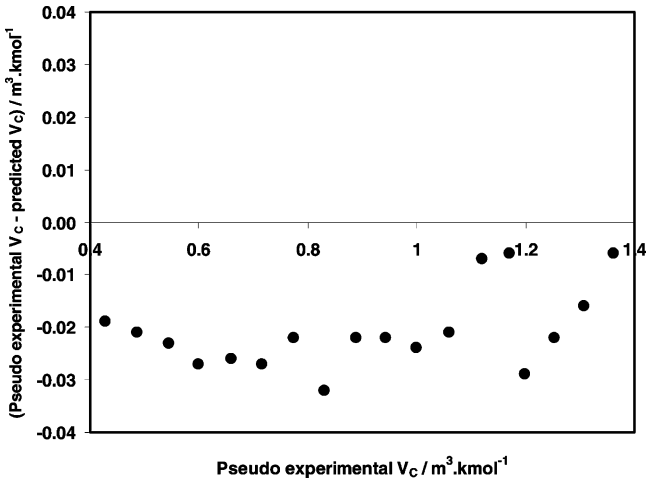

Figure 8. Difference between the pseudo-experimental value and the predicted value versus the pseudo-experimental value for critical volume of normal paraffin. (●) data used for validation.

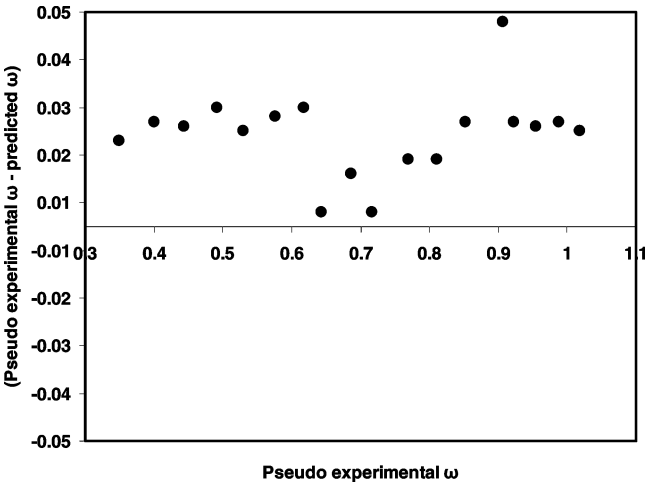

Figure 9. Difference between the pseudo-experimental value and the predicted value versus the pseudo-experimental value for acentric factor of normal paraffin. (●) data used for validation.

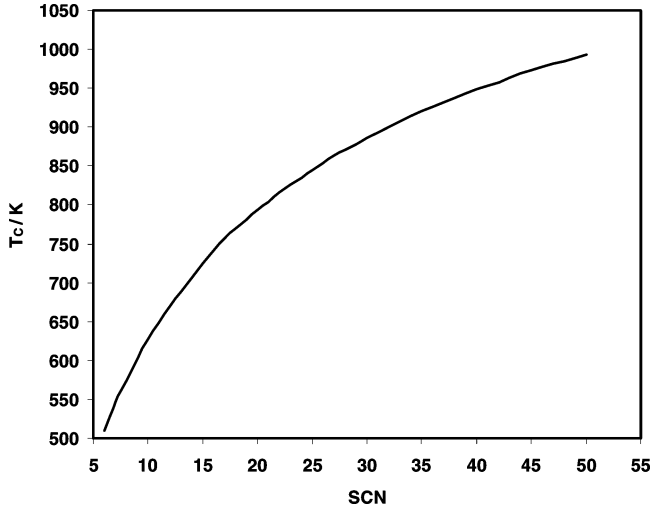

Figure 10. Critical temperature versus SCN.

be seen, the maximum differences between the pseudo-experimental[1] and predicted values are 13 K for the critical temperatures, 0.15 MPa for the critical pressures, less than 0.035 m^3·kmol^{-1} for the critical volumes, and less than 0.05 for the acentric factors. It should be mentioned that although the maximum difference between the pseudo-experimental[1] and predicted critical temperatures seems relatively high (13 K), it can be considered acceptable due to uncertainty in estimating critical temperatures of heavy hydrocarbons.

Figures 10 −13 show the estimated values of the critical temperatures, critical pressures, critical volumes, and acentric factors, respectively, for SCNs from C_6 to C_{50}. As can be seen, the ANN model correctly determines the critical properties and acentric factors of the SCNs for the practical applications ranges (C_1 to C_{50}), even for SCNs not used in training the model (i.e., C_{45} to C_{50}). At high SCNs, the values of the critical properties and the acentric factors become weak functions of the SCNs and approach special values. As the petroleum fractions heavier than C_{30} have more asphaltenic nature[17,18]

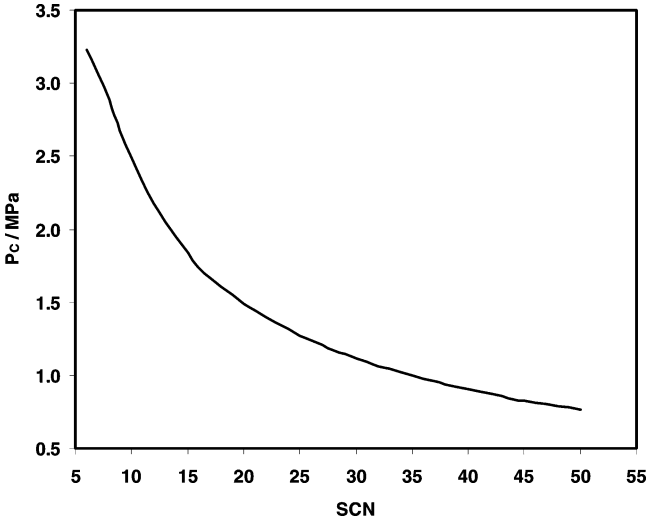

Figure 11. Critical pressure versus SCN.

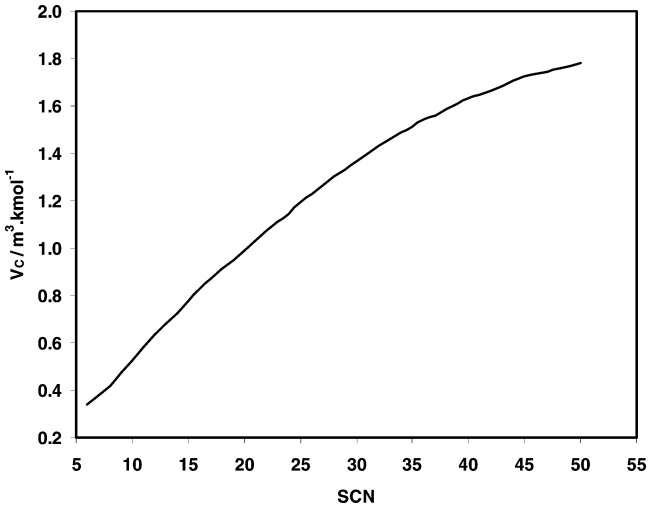

Figure 12. Critical volume versus SCN.

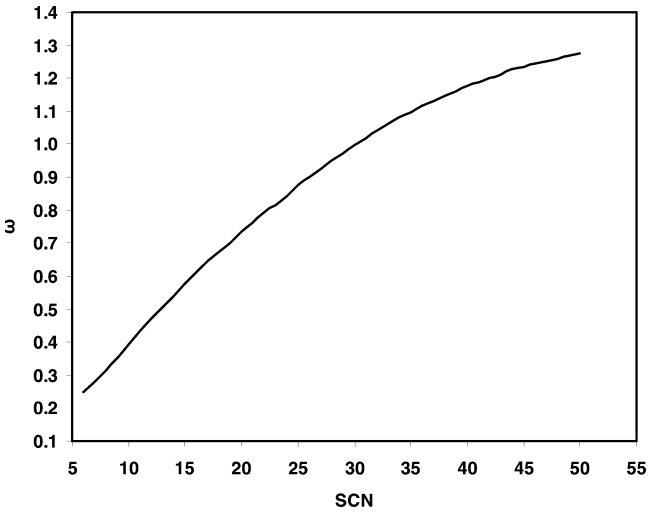

Figure 13. Acentric factor versus SCN.

and asphaltene is the heaviest component of oil, these special values are close to the recommended values reported in the literature[18] for the critical properties and the acentric factors of asphaltene. Finally, it should be mentioned that the ANN model developed in this work, like other correlations reported in the literature,[1] is recommended to use for petroleum fractions properties, and its application to very wide boiling-point range fractions, such as C_{7+} is not recommended.

4. Conclusions

In this work, a brief review was first made on the most common correlations reported in the literature for determining the critical properties and acentric factors of petroleum fractions. The study showed a need for developing a new method for estimating these properties, especially for heavy petroleum fractions. A feed-forward artificial neural network model was then developed to determine the critical temperatures, critical pressures, critical volumes, and the acentric factors of C_1-C_{45} petroleum fractions as a function of specific gravities and average normal boiling-points values. The data recommended in the literature on the above-mentioned properties were used to develop this technique. It was shown that the predictions of this model for the critical properties and acentric factors of petroleum fractions are in close agreement with those recommended in the literature.

Appendix

The Most Widely Used or Promising Methods for Determining the Critical Properties and the Acentric Factors of Petroleum Fractions (Information from Ref 1). The units of temperature, pressure, and volume are Rankine, psia, and ft^3/lb·mol, respectively, in all of the following equations. The specific gravity, S, is defined relative to water at 60 °F.

A.1. Lee−Kesler Correlations.

$$T_c = 341.7 + 811S + (0.4244 + 0.1174\,S)T_b + (0.4669 - 3.2623\,S) \times 10^5/T_b$$

$$\ln P_c = 8.3643 - 0.0566/S - (0.24244 + 2.2898/S + 0.11857/S^2) \times 10^{-3}\,T_b + (1.4685 + 3.648/S + 0.47227/S^2) \times 10^{-7}\,T_b^2 - (0.42019 + 1.6977/S^2) \times 10^{-10}\,T_b^3$$

$$\omega = (\ln P_{br} - 5.92714 + 6.09648/T_{br} + 1.28862 \ln T_{br} - 0.169347T_{br}^6)/(15.2518 - 15.6875/T_{br} - 13.4721 \ln T_{br} + 0.4357T_{br}^6) \quad \text{for } T_{br} \le 0.8$$

$$\omega = -7.904 + 0.1352\,K_w - 0.007465\,K_w^2 + 8.359T_{br} + (1.408 - 0.01063\,K_w)/T_{br} \quad \text{for } T_{br} > 0.8$$

where $P_{br} = P_b/P_c$, $T_{br} = T_b/T_c$; P_b is the pressure at which T_b is measured, for example, the average normal boiling point temperature at 14.69 psia, and K_w is the Watson characterization factor $K_w = T_b^{1/3}/S$

A.2. Cavett Correlations.

where API = (141.5/S) − 131.5.

A.3. Riazi-Daubert Correlations.

$$\theta = a\,[\exp(b\theta_1 + c\theta_2 + d\,\theta_1\,\theta_2)]\,\theta_1^{\,e}\,\theta_2^{\,f}$$

where $a-f$ are constants for each property, which are given in Table A.1.

A.4. Twu Correlations. The method initially correlates the properties of normal paraffins as the reference. The calculated values are then adjusted for petroleum fractions using the difference between the specific gravity of the hydrocarbon

Table A.1: Constants $a-f$ in Riazi−Daubert Correlations[1] ($70 < M < 300$ and $540 < T_b < 1110$ °R)

θ	θ_1	θ_2	a	b	c	d	e	f
T_c	T_b	S	10.6443	−0.00051747	−0.54 444	0.00035995	0.81067	0.53691
T_c	M	S	554.4	−0.00013478	−0.61 641	0.0	0.2998	1.0555
P_c	T_b	S	6 162 000	−0.004725	−4.8014	0.0031939	−0.4844	4.0846
P_c	M	S	45 203	−0.0018078	−0.3084	0.0	−0.8063	1.6015
(V_c/M)	T_b	S	0.0006233	−0.0014679	−0.26404	0.001095	0.7506	−1.2028
(V_c/M)	M	S	0.01206	−0.002657	0.5287	0.0026012	0.20378	−1.3036
M	T_b	S	581.96	0.00054308	−9.53384	0.00111056	0.97476	6.51274
T_b	M	S	6.77856	0.00377406	2.984036	−0.00425288	0.401673	−1.58256

(4)

$$T_c = 768.071 + 1.7134\,(T_b - 459.67) - 0.10834 \times 10^{-2}\,(T_b - 459.67)^2 + 0.3889 \times 10^{-6}\,(T_b - 459.67)^3 - 0.89213 \times 10^{-2}\,(T_b - 459.67)\,\mathrm{API} + 0.53095 \times 10^{-5}\,(T_b - 459.67)^2\,\mathrm{API} + 0.32712 \times 10^{-7}\,(T_b - 459.67)^2\,\mathrm{API}^2$$

$$\log P_c = 2.829 + 0.9412 \times 10^{-3}\,(T_b - 459.67) - 0.30475 \times 10^{-5}\,(T_b - 459.67)^2 + 0.15184 \times 10^{-8}\,(T_b - 459.67)^3 - 0.20876 \times 10^{-4}\,(T_b - 459.67)\,\mathrm{API} + 0.11048 \times 10^{-7}\,(T_b - 459.67)^2\,\mathrm{API} - 0.4827 \times 10^{-7}\,(T_b - 459.67)\,\mathrm{API}^2 + 0.1395 \times 10^{-9}\,(T_b - 459.67)^2\,\mathrm{API}^2$$

fraction and that of the normal paraffin with the same boiling point as the correcting parameter.

Normal Paraffins. The properties of normal paraffins are correlated with the average normal boiling-point temperature,

$$T_{cp} = T_b\,[0.533272 + 0.191017 \times 10^{-3}\,T_b + 0.779681 \times 10^{-7}\,T_b{}^2 - 0.284376 \times 10^{-10}\,T_b{}^3 + 0.959468 \times 10^2/(T_b/100)^{13}]^{-1}$$

$$P_{cp} = (3.83354 + 1.19629\Psi^{1/2} + 34.8888\Psi + 36.1952\Psi^2 + 104.193\Psi^4)^2$$

$$V_{cp} = [1 - (0.419869 - 0.505839\Psi - 1.56436\Psi^3 - 9481.70\Psi^{14})\,]^{-8}$$

$$S_p = 0.843593 - 0.128624\Psi - 3.36159\Psi^3 - 13749.5\Psi^{12}$$

where subscript p refers to the properties of paraffins and

$$\Psi = 1 - T_b/T_{cp}$$

The molecular weight of paraffins is given by the following implicit relation,

$$T_b = \exp[5.71419 + 2.71579 \ln M_p - 0.286590\,(\ln M_p)^2 - 39.8544/(\ln M_p) - 0.122488/(\ln M_p)^2\,] - 24.7522 \ln M_p + 35.3155\,(\ln M_p)^2$$

which can be solved iteratively using the following guess,

$$M_p = T_b/(10.44 - 0.0052T_b)$$

Petroleum Fractions. The properties of any petroleum fraction are estimated by adjusting the calculated properties of the normal paraffin with the same boiling point temperature as,

Critical Temperature:

$$T_c = T_{cp}\,[(1 + 2f_T)/(1 - 2f_T)]^2$$

$$f_T = \Delta S_T\,[-0.362456/T_b{}^{1/2} + (0.0398285 - 0.948125/T_b{}^{1/2})\Delta S_T]$$

$$\Delta S_T = \exp[5\,(S_P - S)] - 1$$

Critical Volume:

$$V_c = V_{cp}\,[(1 + 2f_v)/(1 - 2f_v)]^2$$

$$f_v = \Delta S_v\,[0.466590/T_b{}^{1/2} + (-0.182421 + 3.01721/T_b{}^{1/2})\,\Delta S_v]$$

$$\Delta S_v = \exp[4(S_P{}^2 - S^2)] - 1$$

Critical Pressure:

$$P_c = P_{cp}(T_c/T_{cp})(V_{cp}/V_c)[(1 + 2f_p)/(1 - 2f_p)]^2$$

$$f_p = \Delta S_p\,[(2.53262 - 46.1955/T_b{}^{1/2} - 0.00127885\,T_b) + (-11.4277 + 252.140/T_b{}^{1/2} + 0.00230535\,T_b)\Delta S_p]$$

$$\Delta S_p = \exp[0.5(S_p - S)] - 1$$

Molecular Weight:

$$\ln M = (\ln M_p)[(1 + 2\,f_M)/(1 - 2\,f_M)]^2$$

$$f_M = \Delta S_M\,[|\Psi| + (-0.0175691 + 0.193168/T_b{}^{1/2})\Delta S_M]$$

$$\Psi = 0.0123420 - 0.328086/T_b{}^{1/2}$$

$$\Delta S_M = \exp[5(S_p - S)] - 1$$

Acknowledgment

Waheed Afzal wishes to thank the Higher Education Commission of Pakistan for financial support.

Literature Cited

(1) Danesh, A. *PVT and Phase Behaviour of Petroleum Reservoir Fluids*; Elsevier Science B.V.: The Netherlands, 2007.

(2) Ahmed, T. *Hydrocarbon Phase Behaviour*; Gulf Publishing Company: Houston, 1989 (quoted in ref 1).

(3) Rivollet, F. Etude des Propriétés Volumétriques (PVT) d'Hydrocarbures Légers (C1−C4), du Dioxyde de Carbone et de l'Hydrogène Sulfuré: Mesures par Densimétrie à Tube Vibrant et Modélisation, Ph.D. thesis, Ecole des Mines de Paris (Paris School of Mines), France, December 2005 (in French).

(4) Wilamowski, B.; Iplikci, S.; Kayank, O. and Efe, M. O. An Algorithm for Fast Convergence in Training Neural Networks, International Joint Conference on Neural Networks (IJCNN′01), Washington D.C., July, 2001; pp 1778−1782.

(5) Marquardt, D. An Algorithm for Least-Squares Estimation of Nonlinear Parameters. *SIAM J. Appl. Math.* **1963**, *11*, 431−441.

(6) Levenberg, K. A Method for the Solution of Certain Problems in Least Squares. *Quart. Appl. Math*. **1944**, *2*, 164−168.

(7) Chouai, A.; Laugier, S. and Richon, D. Modeling of Thermodynamic Properties Using Neural Networks: Application to Refrigerants. *Fluid Phase Equilib*. **2002**, *199*, 53−62.

(8) Piazza, L.; Scalabrin, G.; Marchi, P. and Richon, D. Enhancement of the Extended Corresponding States Techniques for Thermodynamic Modelling. I. Pure fluids. *Int. J. Refrig.* **2006**, *29*, 1182−1194.

(9) Scalabrin, G.; Marchi, P.; Bettio, L. and Richon, D. Enhancement of the Extended Corresponding States Techniques for Thermodynamic Modelling. II. Mixtures. *Int. J. Refrig.* **2006**, *29*, 1195−1207.

(10) Schmitz, J. E.; Zemp, R. J. and Mendes, M. J. Artificial Neural Networks for the Solution of the Phase Stability Problem. *Fluid Phase Equilib.* **2006**, *245*, 83−87.

(11) Elgibaly, A. A. and Elkamel, A. M. A New Correlation for Predicting Hydrate Formation Conditions for Various Gas Mixtures and Inhibitors. *Fluid Phase Equilib.* **1998**, *152*, 23−42.

(12) Chapoy, A.; Mohammadi, A. H. and Richon, D. Predicting the Hydrate Stability Zones of Natural Gases Using Artificial Neural Networks. *Oil & Gas Science and Technology − Rev. IFP*. 2007, 62/15, 701−706.

(13) Mohammadi, A. H. and Richon, D. Estimating the Hydrate Safety Margin in the Presence of Salt or Organic Inhibitor Using Refractive Index Data of Aqueous Solution. *Ind. Eng. Chem. Res*. **2006**, *45*, 8207−8212.

(14) Mohammadi, A. H. and Richon, D. Determination of Gas Hydrate Safety Margin Using Specific Gravity Data of Salt or Organic Inhibitor Aqueous Solution. *Ind. Eng. Chem. Res.* **2007**, *46*, 3852−3857.

(15) Mohammadi, A. H.; Martínez-López, J. F. and Richon, D. Determination of Hydrate Stability Zone Using Electrical Conductivity Data of Salt Aqueous Solution. *Fluid Phase Equilib.*. **2007**, *253*, 36−41.

(16) Mohammadi, A. H.; Martínez-López, J. F. and Richon D. Predicting Hydrate Stability Zones of Petroleum Fluids Using Sound Velocity Data of Salt Aqueous Solutions. *Fluid Phase Equilib.* **2007**, *253*, 165−170.

(17) Nghiem, L. X.; Hassam, M. S.; Nutakki, R. and George, A. E. D. Efficient Modelling of Asphaltene Precipitation, SPE 26642, SPE Annual Technical Conference and Exhibition, Houston, Texas, October 3−6, 1993.

(18) Firoozabadi A. *Thermodynamics of Hydrocarbon Reservoirs*, 1st ed.; McGraw-Hill: New York, 1999.

Received for review September 12, 2007
Revised manuscript received February 15, 2008
Accepted February 26, 2008

IE0712378